Oligonucleotides

DOI: 10.1002/anie.201104382

Interplay between “Neutral” and “Charge-Transfer” Excimers Rules the Excited State Decay in Adenine-Rich Polynucleotides**

Roberto Improta and Vincenzo Barone*

The biological relevance of UV light absorption by DNA (which can lead to genetic code damages) explains the strong scientific interest in the excited-state dynamics of polynucleotides.[1–6] Although studies on adenine(A)-based oligonucleotides as $(dA)_n$ and $(dA)_n(dT)_n$[7–22] (T: thymin) have surely provided fundamental insights, several very basic issues are still matter of a lively debate.[2–6] For example, the slowest time decay components have been alternatively assigned to charge-transfer (CT) exciplexes,[2] to neutral A excimers,[17] to excitons delocalized on multiple bases,[8] or even to long-living monomer-like excited states.[18] More generally, a comprehensive picture of the absorption and the decay process is still lacking. To clarify those issues, we have performed a full quantum-mechanical study in aqueous solution of the lowest energy singlet electronic states of a realistic model of poly(dA): $(dA)_4Na_3$ (see Figure 1). Fully relaxed excited-state geometry optimizations allowed to identify all the minima responsible for the most prominent spectral features, thus enabling to characterize all the main excited-state decay paths of $(dA)_n$ on the same foot and to propose an explanation of all the spectroscopic results.

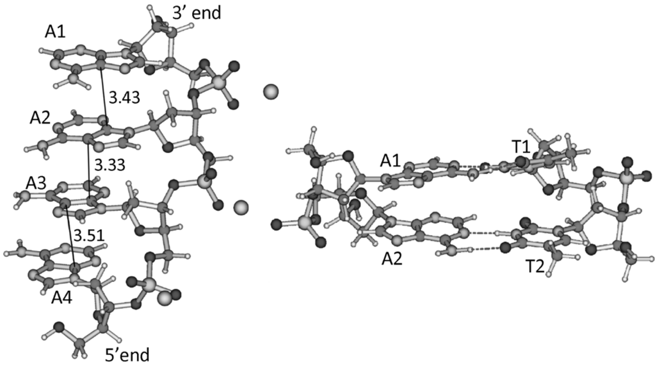

Figure 1. Schematic drawing of systems investigated in the present study; left: $(dA)_4Na_3$ (the stacking distance in the ground-state minimum according to PCM/M052X calculations in water is also noted); right: $(dA)_2{\cdot}(dT)_2$.

Our investigation is rooted in time-dependent density functional theory (TD-DFT),[23] mainly using the hybrid M052X[24] functional, which has been tailored to treat stacked systems and correctly describe CT transitions, and double-checking the main conclusions by using three additional functionals, M062X,[24] CAM-B3LYP,[25] and PBE0.[26] We included solvent effects by the polarizable continuum model (PCM),[27] also exploiting the very accurate state specific (SS) version of PCM/TD-DFT.[28] Despite the absence of explicit water molecules, previous studies have convincingly shown that this approach can reliably describe solvent effects on the excited-state decay[19,20] (see the Supporting Information for details). A further validation is provided by the computed absorption and electronic circular dichroism spectra of $(dA)_4Na_3$ (see the Supporting Information), which reproduce their experimental counterparts well.[19–21] Though additional tuning of the results for longer DNA motifs can be induced by helix fluctuations,[22] the essential characteristics of the phenomenon should be captured by our $(dA)_4Na_3$ model.

The lowest-energy absorption band of $d(A)_n$ is caused by an exciton delocalized over multiple bases[19,20] (originated by the combinations of the HOMO→LUMO transitions, L_a, of the different monomers),[29] although with major contributions from A dimers. As discussed in the Supporting Information, though TD-DFT and CASPT2[17] agree in predicting excitons delocalized over two bases red-shifted by approximately 0.25 eV with respect to the main absorption band, absorption in the UVA (especially for $\lambda > 300$ nm)[11] is due to A→A CT states. These latter states are characterized in water by energies comparable to those of the bright excitons and by large inhomogeneous broadenings (see the Supporting Information).

We have performed several full geometry optimization runs of $(dA)_4Na_3$, starting from different structures, using both M052X and PBEO functionals and both at the solvent equilibrium (eq) and nonequilibrium (neq) levels of the 8 lowest-energy excited states (see the Supporting Information for details). We summarize herein the main minima/decay paths unveiled by our analysis (see Figure 2), following excitation at approximately 265 nm, when most of the initial excited-state population is associated with bright excitons. In general, the potential energy surfaces (PES) associated with each decay path are rather flat, are characterized by multiple crossings (all the minima described below correspond to relative minima of the lowest energy adiabatic excited state,

---

[*] Dr. R. Improta
CNR-Consiglio Nazionale delle Ricerche
Istituto di Biostrutture Biommagini (IBB-CNR)
Via Mezzocannone 16, 80136, Napoli (Italy)
E-mail: robimp@unina.it
Prof. V. Barone
Scuola Normale Superiore, Piazza dei Cavalieri, 7 56126 Pisa (Italy)

[**] The authors would like to thank Dr. D. Markovitsi and Dr. A. Banyasz for very useful discussion and for giving access to several unpublished results. R.I. thanks Laboratoire Francis Perrin (CNRS) for hospitality and MIUR (PRIN 2008 and FIRB Futuro in Ricerca) for financial support.

Supporting information for this article is available on the WWW under http://dx.doi.org/10.1002/anie.201104382.

© 2011 Wiley-VCH Verlag GmbH & Co. KGaA, Weinheim

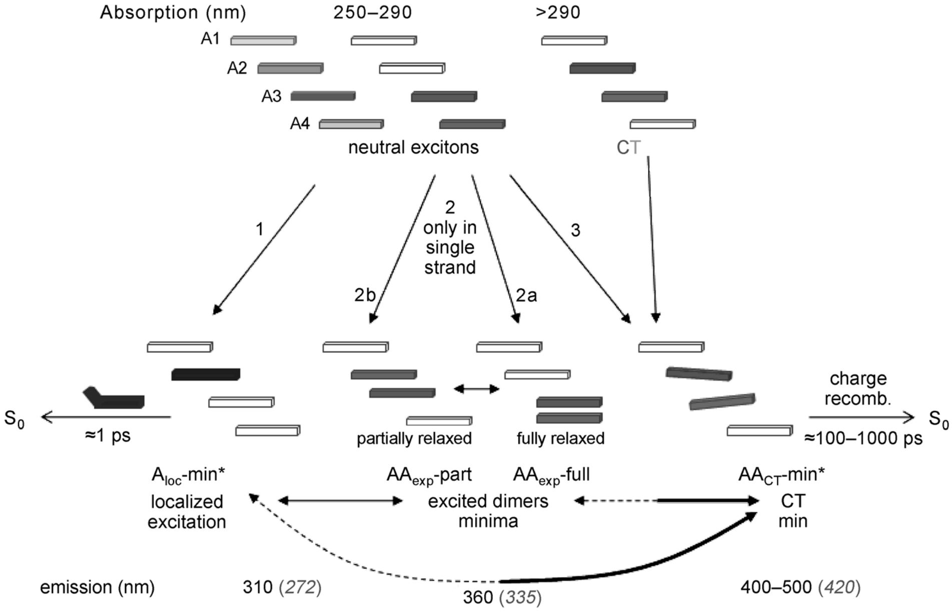

Figure 2. Schematic drawing of the main excited-state decay routes in d(A)$_n$ single strands, modeled by a d(A)$_4$ tetranucleotide. Each bar schematically represents an A base, while the intensity of the color is proportional to the participation of the base in the electronic transition. Experimental and computed (in parentheses, SS-PCM/TD-M052X/6-31G(d) calculations) emission energies are also reported.

S$_1$), and are significantly modulated by dynamical solvent effects.

Sudden localization of the excitation on a single base is possible, as experimentally found in mixed-sequence polynucleotides,[30] while the system passes through a plateau (energy gradient approximately 0.002 a.u., A$_{loc}$-min*, see Table 1), where the purine ring keeps a planar geometry (path **1** in Figure 2). A$_{loc}$-min* pseudo-minimum, with a computed emission energy (ν_{em}) of approximately 4.5 eV (275 nm; i.e. with a similar Stokes shift to that of fluorescence from isolated A) accounts for most of the monomer-like emission ($\lambda_{em}^{exp} \approx$ 310 nm), which decays on a fast scale;[16] it is connected to another plateau characterized by a strongly pyramidalized C2 atom (A$_{loc}$-pyr, see Figure 3) by a barrierless path. In the A monomer, C2 pyramidalization is accompanied by a simultaneous out-of-plane motion of the H2 atom while a very steep path leads to a conical intersection (CI) with S$_0$.[29] Such a process appears more difficult within the single strand.[18] However, our calculations (see the Supporting Information) suggest that, if an energy barrier in the path towards the CI exists, its height is extremely low (< 0.05 eV). Furthermore, both A$_{loc}$-min* and A$_{loc}$-pyr are significantly less stable than the other excited-state minima of (dA)$_4$Na$_3$. We can conclude, in agreement with previous studies,[3] that the long-living components of dA$_n$ are not associated to this decay path. The less steep path towards the CI with S$_0$,[31] together with the time necessary for the localization process, gives account of the slight slowing down of the decay rate at 310 nm with respect to adenosine monophosphate.[16,31] A very recent dynamical study agrees in predicting a decay time on the picosecond range for the monomer-like path, though suggesting the possible involvement of nπ* excitation.[22]

Table 1: Oscillator strength (Osc), relative adiabatic energies (AE) in eV with respect to the ground-state minimum, and emission energies (ν_{em}) of the lowest-energy excited states of (dA)$_4$Na$_3$ in their respective minima.[a]

Description	Path 2		Path 3	Path 1	
	AA$_{exc}$-full	AA$_{exc}$-part	AA$_{CT}$-min*	A$_{loc}$-min*	A$_{loc}$-pyr
			M052X		
Osc.	0.00	0.02	0.00	0.14	0.04
AE	4.35	4.55	4.05	4.97	4.76
ν_{em}	3.70	3.87	2.95	4.56	3.38
			M062X		
Osc.	0.00	0.01	0.00	0.13	0.04
AE	4.23	4.45	4.06	4.89	4.71
ν_{em}	3.69	3.87	2.88	4.51	3.36
			PBE0		
Osc.	0.00	0.02	0.00	[b]	0.04
AE	4.18	4.39	2.81		4.51
ν_{em}	3.37	3.52	2.09		3.22
			CAM-B3LYP		
Osc.	0.00	0.01	0.00	0.14	0.04
AE	4.55	4.77	3.69	4.94	4.70
ν_{em}	3.69	3.85	2.88	4.50	3.39

[a] Equilibrium SS-PCM/TD-DFT/6-31G(d) calculations on LR-PCM/TD-M052X/6-31G(d) optimized geometries in aqueous solution. Additional details can be found in the Supporting Information; [b] SS-PCM calculations converge to a partially CT excited state.

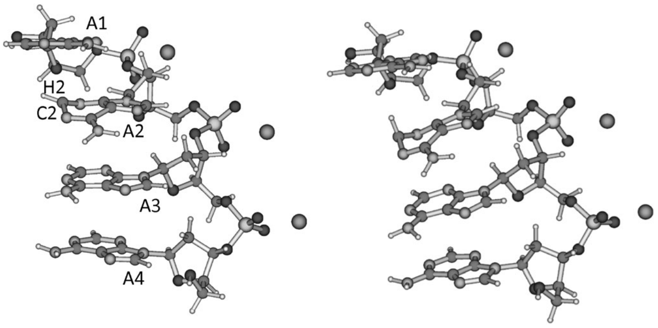

Figure 3. Schematic drawing of left: a representative point (A$_{loc}$-pyr) on the plateau in the path leading to the CI with S$_0$ for the "monomer-like" localized excited state in (dA)$_4$Na$_3$; right: the CI with S$_0$ for A$_{loc}$. PCM/TD-M052X/6-31G(d) computations.

Excitons can also decay towards a "neutral" excimer delocalized on a stacked A dimer (AA$_{exc}$, path **2** in Figure 2). This path is characterized by a decrease of the inter-monomer distance of the two involved bases, shifting towards a more symmetric "face-to-face" stacking arrangement. Concomitantly, the intensity and the wavelength of the ν_{em} decrease.

Two limiting situations exist, represented by two slightly different minima. For "stacked dimers" close to the strand terminus, a steep path leads to a fully relaxed minimum (AA_{exc}-full, see Figure 4), where the excitation is almost perfectly delocalized on the two A bases, characterized by a very short stacking distance and face-to-face arrangement. The structural features are similar to those found for the analogous species in the A dimer by CASPT2 calculations,[17] but strand constraint leads to a significantly less symmetric stacking geometry. ν_{em} is 3.70 eV (335 nm) at the M052X level and 3.37 eV (370 nm) at the PBE0 level, that is, with a Stokes shift of approximately 1.8 eV.

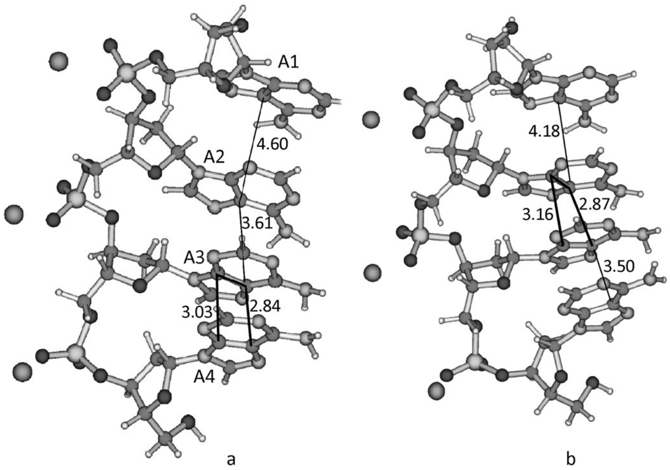

Figure 4. Schematic drawing of the neutral excimer minima according to LR-PCM/TD-M052X calculations in aqueous solution on $(dA)_4Na_3$; left: fully relaxed minimum involving two terminal A bases. The dihedral angle marked in bold is −9.8°; right: partially relaxed minimum involving two "internal" A bases. The dihedral angle marked in bold is −16.1°.

Especially for "internal" dimers (e.g. A2 and A3) "partially relaxed" minima (AA_{exc}-part) exist, where the B-DNA geometry is less distorted than in AA_{exc}-full. The system is predicted to be trapped in a wide plateau, where structures corresponding to partially delocalized excimers, characterized by a relatively intense emission around approximately 4.1 eV (300 nm), are very close in energy to delocalized minima weakly emitting around 3.9 eV (320 nm). The dynamical behavior of AA_{exc} is complex, involving both very fast (the formation of the excimer and the initial decrease of stacking distance) and slower (the motion on the plateau involving substantial rearrangement of the backbone) degrees of freedom. These features, together with the computed Stokes shift, are fully consistent with the very broad fluorescence spectra of $(dA)_{20}$, centred at $\lambda_{em}^{exp} \approx 360$ nm, and its complex multi-exponential decay. Since formation of A–A photodimers is not likely, besides to emission to S_0, the decay of AA_{exc} should proceed through paths **1** and **3**.

Test calculations on $(dA)_2 \cdot (dT)_2$ (see the Supporting Information) indicate that base pairing strongly decreases the relative importance of decay path **2**, involving severe distortions of the stacking geometry. Experimental fluorescence spectra of AT double strands, dominated by emission stemming from thymine,[12] indeed do not show any sign of the 360 nm band. Minima like AA_{exc}-full could instead play an important role in the excited-state decay of smaller and less hindered systems like $(dA)_2$.[15]

To not overemphasize solvent effects, we focus on the CT excited state formed by the two internal A bases (path **3** in Figure 2) that are less exposed to solvent than terminal A, by exploiting PCM/TD-PBE0/6-31G(d) calculations, allowing an easier optimization of CT states (see the Supporting Information). SS-PCM/TD-M052X/6-31G(d) calculations indicate that at the solvent eq level the CT minimum (AA_{CT}-min*) is the absolute excited-state minimum, ν_{em} being 2.98 eV (ca. 415 nm). Although the transition exhibits a clear-cut CT character (involving the transfer of ca. 0.8 a.u.), due to the residual overlap between the molecular orbitals (MO) of the two A bases (the stacking distance of which is still ca. 3.6 Å), the electronic transition is weak but not completely dark. Emission from AA_{CT}-min* is very broad, due to the large associated inhomogeneous broadening. It should be responsible for the component/shoulder around $\lambda_{em}^{exp} = 420$ nm in the steady-state spectrum of A_{20}.[12] The strong anisotropy decrease found for $\lambda_{em}^{exp} = 420$ nm, which is larger than that found for smaller wavelengths, supports our suggestion that emission at 420 nm is mainly associated to the CT state.[12]

After absorption to different exciton states delocalized over multiple A bases, our calculations show that the dynamics are ruled by three species responsible for different spectral features: bright excited states localized on a single monomer (path **1**), darker "neutral excimers" (path **2**), or CT exciplexes (path **3**) that represent the most stable minima. As discussed in the Supporting Information, several experimental[6,16,30] and computational[32] results together with the analysis of the computed PES, strongly suggest that the three decay routes coexist from the very beginning of the excited-state dynamics and that they are in dynamic equilibrium. Especially in the first picosecond after the excitation, solvent and backbone fluctuations can lead to A_{loc}/AA_{exc} and AA_{exc}/AA_{CT} interconversions. For example, quantum dynamical calculations on A stacked dimers[32] indicate that the population transfer between the bright excitonic and the CT states is fast and effective and, at the solvent neq level, fully reversible. A critical role is played by dynamic solvation effects (due to the motion of the solvent molecules and charged moieties of the backbone), which are crucial for the stability of AA_{CT}.

According to our model, emission at different wavelengths is mainly associated with different species, with different lifetimes, explaining why the lifetime increases and the anisotropy decreases when monitoring fluorescence in the range of 300–420 nm.[12,16] Conversely, the relative weight of the different excited states and, therefore, of the possible decay paths, also depends on the excitation wavelength. For example, excitation in the UVA essentially produces AA_{CT} states.

The very recent experimental finding that the fluorescence spectra of $(dA)_{20}$, and $(dA)_{20} \cdot (dT)_{20}$ are strongly dependent on excitation wavelengths thus provides a striking validation of our model.[11] Fluorescence spectra recorded

© 2011 Wiley-VCH Verlag GmbH & Co. KGaA, Weinheim

upon UVA excitation of $(dA)_{20}$ and $(dA)_{20}\cdot(dT)_{20}$ indeed show a maximum at $\lambda_{em}^{exp} \approx 420$ nm[11] (the computed emission energy of AA_{CT} is not very sensitive to the formation of the double strand).[19] The very broad shape of the spectrum, with a relatively high contribution also from very long wavelengths (500–600 nm) and its very slow decay ($\langle\tau\rangle = 670$ ps)[11] is also consistent with the emission from a CT state.

Our picture is consistent also with transient absorption experiments on $(dA)_{18}$ and $(dA)_{18}\cdot(dA)_{18}$.[7] While after approximately 10 ps the decay of the signal assigned[7] to the CT state is almost superimposable to that characteristic of ground-state absorption, the decays in the first picoseconds are more strongly wavelength dependent, thus suggesting the participation of additional excited states. Approximately 10% of the initial signal remains 1 ns after the pump pulse, as it happens for the excited state emitting at >400 nm,[11] we indeed assign to a CT state. Our calculations suggest that the decay of the CT state in the single and the double strand is not significantly different: we expect only a larger driving force towards Charge Recombination in the double helix, because of the smaller solvent-exposed surface (a polar solvent stabilizes CT states) and, therefore, a slightly slower decay in consistency with the experimental results.[7,11] The finding that long-living excited states are formed within $(dA)_2$ and that their bleaching recovery does not depend on the number of the stacked bases[14] also fits very well with our model.

For many other stacked bases (e.g. purine/pyrimidine pairs) CT excited states should be even more favored than for AA dimers, suggesting that CT between stacked bases (followed by charge recombination or decay to localized excitations) could be a major, if not the most important, decay route for DNA, representing, for example, the "trapping dark state" responsible for delayed fluorescence in natural DNA.[6] On the other hand, the possibility of "directly" exciting CT states and/or the effectiveness of the decay of the "neutral" exciton to CT state can significantly depend on the excitation wavelength, suggesting that the DNA decay could be in principle tuned by suitably shaping the laser pulses.

Received: June 24, 2011
Revised: September 23, 2011
Published online: October 25, 2011

Keywords: computational chemistry · DNA · excited states · nucleobases · oligonucleotides

---

[1] C. E. Crespo-Hernández, B. Cohen, P. M. Hare, B. Kohler, *Chem. Rev.* **2004**, *104*, 1977 – 2020.
[2] C. T. Middleton, K. de La Harpe, C. Su, Y. K. Law, C. E. Crespo-Hernández, B. Kohler, *Annu. Rev. Phys. Chem.* **2009**, *60*, 13 – 47.
[3] B. Kohler, *J. Phys. Chem. Lett.* **2010**, *1*, 2047 – 2053.
[4] D. Markovitsi, T. Gustavsson, I. Vayá, *J. Phys. Chem. Lett.* **2010**, *1*, 3271 – 3276.
[5] N. K. Schwalb, F. Temps, *Science* **2008**, *322*, 243 – 245.
[6] I. Vayá, T. Gustavsson, F. A. Miannay, T. Douki, D. Markovitsi, *J. Am. Chem. Soc.* **2010**, *132*, 11834 – 11835.
[7] C. E. Crespo-Hernández, B. Cohen, B. Kohler, *Nature* **2005**, *436*, 1141 – 1144.
[8] D. Markovitsi, F. Talbot, T. Gustavsson, D. Onidas, E. Lazzarotto, S. Marguet, *Nature* **2006**, *441*, E7.
[9] I. Buchvarov, Q. Wang, M. Raytchev, A. Trifonov, T. Fiebig, *Proc. Natl. Acad. Sci. USA* **2007**, *104*, 4794 – 4797.
[10] S. Tonzani, G. C. Schatz, *J. Am. Chem. Soc.* **2008**, *130*, 7607 – 7612.
[11] A. Banyasz, I. Vayá, P. Changenet-Barret, T. Gustavsson, T. Douki, D. Markovitsi, *J. Am. Chem. Soc.* **2011**, *133*, 5163 – 5165.
[12] D. Onidas, T. Gustavsson, E. Lazzarotto, D. Markovitsi, *J. Phys. Chem. B* **2007**, *111*, 9644 – 9650.
[13] D. Markovitsi, D. Onidas, T. Gustavsson, F. Talbot, E. Lazzarotto, *J. Am. Chem. Soc.* **2005**, *127*, 17130 – 17131.
[14] T. Takaya, C. Su, K. de La Harpe, C. E. Crespo-Hernández, B. Kohler, *Proc. Natl. Acad. Sci. USA* **2008**, *105*, 10285 – 10290.
[15] M. C. Stuhldreier, C. Schüler, J. Kleber, F. Temps in *Ultrafast Phenomena XVII* (Eds.: M. Chergui, D. Jonas, E. Riedle, R. W. Schoenlein, A. Taylor), Oxford University Press, in press.
[16] W.-M. Kwok, C. Ma, D. L. Phillips, *J. Am. Chem. Soc.* **2006**, *128*, 11894 – 11905.
[17] G. Olaso-González, M. Merchán, L. Serrano-Andrés, *J. Am. Chem. Soc.* **2009**, *131*, 4368 – 4377.
[18] I. Conti, P. Altoe, M. Stenta, M. Garavelli, G. Orlandi, *Phys. Chem. Chem. Phys.* **2010**, *12*, 5016 – 5023.
[19] F. Santoro, V. Barone, R. Improta, *J. Am. Chem. Soc.* **2009**, *131*, 15232 – 15245.
[20] F. Santoro, V. Barone, R. Improta, *ChemPhysChem* **2008**, *9*, 2531 – 2537.
[21] F. Santoro, V. Barone, R. Improta, *Proc. Natl. Acad. Sci. USA* **2007**, *104*, 9931 – 9937.
[22] Y. Lu, Z. Lan, W. Thiel, *Angew. Chem.* **2011**, *123*, 6996 – 6999; *Angew. Chem. Int. Ed.* **2011**, *50*, 6864 – 6867.
[23] K. Burke, J. Werschnik, E. K. U. Gross, *J. Chem. Phys.* **2005**, *123*, 062206.
[24] Y. Zhao, D. G. Truhlar, *Acc. Chem. Res.* **2008**, *41*, 157 – 167.
[25] T. Yanai, D. P. Tew, N. C. Handy, *Chem. Phys. Lett.* **2004**, *393*, 51 – 55.
[26] C. Adamo, V. Barone, *J. Chem. Phys.* **1999**, *110*, 6158 – 6170.
[27] J. Tomasi, B. Mennucci, R. Cammi, *Chem. Rev.* **2005**, *105*, 2999 – 3094.
[28] R. Improta, M. J. Frisch, G. Scalmani, V. Barone, *J. Chem. Phys.* **2007**, *127*, 074504.
[29] I. Conti, M. Garavelli, G. Orlandi, *J. Am. Chem. Soc.* **2009**, *131*, 16108.
[30] K. de La Harpe, B. Kohler, *J. Phys. Chem. Lett.* **2011**, *2*, 133 – 138.
[31] D. Nachtigallová, T. Zeleny, M. Ruckenbauer, T. Muller, M. Barbatti, P. Hobza, H. Lischka, *J. Am. Chem. Soc.* **2010**, *132*, 8261 – 8262.
[32] R. Improta, F. Santoro, V. Barone, A. Lami, *J. Phys. Chem. A* **2009**, *113*, 15346 – 15354.

© 2011 Wiley-VCH Verlag GmbH & Co. KGaA, Weinheim